HMG Advance Access published December 22, 2004

Friedreich ataxia, the oxidative stress paradox

Hervé Seznec[1]*, Delphine Simon[1]*, Cécile Bouton[2], Laurence Reutenauer[1], Ariane Hertzog[1], Pawel Golik[3], Vincent Procaccio[3], Manisha Patel[4], Jean-Claude Drapier[2], Michel Koenig[1] and Hélène Puccio[1].

[1] Institut de Génétique et de Biologie Moléculaire et Cellulaire (IGBMC), CNRS/INSERM/Université Louis Pasteur, 67404 Illkirch cedex, CU de Strasbourg, France.
[2] Institut de Chimie des Substances Naturelles (ICSN), CNRS, avenue de la Terrasse, 91190 Gif-sur-Yvette, France.
[3] Center for Molecular and Mitochondrial Medicine and Genetics (MAMMAG), University of California Irvine, Irvine, CA 92697, USA.
[4] Department of Pharmaceutical Sciences, 4200 East Ninth Avenue, Box C238. University of Colorado Health Sciences Center. Denver CO 80262.

Correspondence should be addressed to HP, IGBMC, 1 rue Laurent Fries BP 10142, 67404 Illkirch, France. Phone: +33-3-8865 3264; Fax: +33-3-8865 3246; hpuccio@igbmc.u-strasbg.fr

*The authors wish it to be known that, in their opinion, the first two authors should be regarded as joint First Authors.

ABSTRACT

Friedreich ataxia (FRDA) results from a generalized deficiency of mitochondrial and cytosolic iron-sulfur protein activity initially ascribed to mitochondrial iron overload. Recent *in vitro* data suggest that frataxin is necessary for iron incorporation in [Fe-S] cluster (ISC) and heme biosynthesis. In addition, several reports suggest that continuous oxidative damage resulting from hampered superoxide dismutases (SODs) signaling participates in the mitochondrial deficiency and ultimately the neuronal and cardiac cell death. This has led to the use of antioxidants as idebenone for FRDA therapy. To further discern the role of oxidative stress in FRDA pathophysiology, we have tested the potential effect of increased antioxidant defense using an MnSOD mimetic (MnTBAP) and Cu,ZnSOD overexpression on the murine FRDA cardiomyopathy. Surprisingly, no positive effect was observed, suggesting that increased superoxide production could not explain by itself the FRDA cardiac pathophysiology. Moreover, we demonstrate that complete frataxin-deficiency does not induce oxidative stress in neuronal tissues nor alters the MnSOD expression and induction in the early step of the pathology (neuronal and cardiac) as previously suggested. We show that cytosolic ISC aconitase activity of IRP-1 progressively decreases while its apo-RNA binding form increases despite the absence of oxidative stress suggesting that in a mammalian system, the mitochondrial ISC assembly machinery is essential for cytosolic ISC biogenesis. In conclusion, our data demonstrate that in FRDA, mitochondrial iron accumulation does not induce oxidative stress and we propose that, contrary to the general assumption, FRDA is a neurodegenerative disease not associated with oxidative damage.

INTRODUCTION

Reactive oxygen species (ROS) are generated during the normal course of metabolism and are important for much physiological functions (for review (1, 2)). However, an excess of ROS can attack a variety of enzymes and has been implicated in lipid peroxidation and protein and DNA oxidation, thereby disrupting cellular functions and integrity. A major intracellular source of ROS is the mitochondrial electron transport chain, with up to 1% of the electron flow leading to the formation of superoxide, $O_2^{\bullet-}$(3, 4). Under normal physiological conditions, the highly reactive $O_2^{\bullet-}$ is rapidly converted within the cell to hydrogen peroxide (H_2O_2) by the superoxide dismutases, Cu,ZnSOD (cytosolic; SOD1) and MnSOD (mitochondrial; SOD2) (5, 6). However, in the presence of reduced transition metals such as iron,, H_2O_2 produces via Fenton reaction the highly reactive and damaging hydroxyl radical, $OH^{\bullet}$ (7). To limit the availability of H_2O_2 for Fenton reaction, detoxifying enzymes such as glutathione peroxidase and catalase exist in distinct cellular compartments (8). In addition, some cellular antioxidants, such as α-tocopherol, ascorbic acid, and glutathione, can directly react with ROS. An imbalance between free radical formation and antioxidant defense mechanism leads to oxidative stress. Thus, it is apparent that oxidative stress induced injury results from the overproduction of oxidants (either through a dysfunctional mitochondria (endogenous) or from exposure to cytotoxic drugs (exogenous)) and/or the dysfunction of endogenous antioxidant defenses.

Oxidative stress and mitochondrial dysfunction have been linked to neurodegenerative disorders such as Alzheimer's disease (9, 10), Parkinson's disease (11), Amyotrophic Lateral Sclerosis (12) and Friedreich Ataxia (13-15). Friedreich ataxia (FRDA) is the most common form of autosomal recessive ataxia and is characterized by degeneration of the large sensory neurons extending into the spinal cord, cardiomyopathy and increased incidence of diabetes (16). The disease is caused by severely reduced levels of frataxin due to a large GAA triplet repeat expansion within the first intron of the frataxin gene (17), causing inhibition of transcriptional elongation. Although substantial progress has been made since the discovery of the gene encoding frataxin, the exact function of frataxin and the mechanisms by which its insufficiency leads to defects in Fe/S cluster (ISC) protein assembly/activity (15, 18), mitochondrial iron deposits (19-22), and alteration in defense against oxidative stress (23-25) are still controversial. Most recent data lean towards a role of frataxin as an iron chaperone closely involved in ISC assembly/protection and heme biosynthesis (13, 26-32).

A long-standing hypothesis is that FRDA is due to an iron-mediated oxidative stress. Early studies showed iron deposits in cardiac tissue of FRDA patients and in the yeast strain deleted for frataxin (Δ*YFH1*) thereby linking impaired iron homeostasis to the disease (19-22). In addition, the specific activities of enzymes that contain Fe-S clusters (ISCs) such as the mitochondrial complex I-III of the respiratory chain and the mitochondrial and cytosolic aconitases are significantly reduced in the heart of patients (15). Furthermore, cultured fibroblasts from patients as well as Δ*YFH1*-yeast exhibit an increased sensitivity to oxidative stress (20, 21, 33). All together, this has led to the hypothesis that a dysfunctional mitochondrial respiratory chain and elevated levels of mitochondrial iron, as a primary or secondary consequence of frataxin deficiency, could generate cell-damaging superoxide and hydroxyl radicals through Fenton reaction. In support of this, elevated levels of oxidative stress markers, urine 8-hydroxy-2'-deoxyguanosine (24) and serum malondialdehyde (25, 34) (indicative of DNA damage and lipid peroxidation, respectively), have been reported in patients. Furthermore, in cultured cells from FRDA patients challenged with exogenous oxidative stress, superoxide dismutases induction was impaired, possibly making the cells even more prone to oxidative damage (23, 33, 35). This has led to the suggestion that continuous oxidative damage due to an impaired response to oxidative stress could further contribute to mitochondrial deficiency and cell degeneration in the disease. Based on these hypotheses, development of antioxidant therapies for slowing or halting the progression of disease has been pursued (36-40). Particularly, idebenone, an antioxidant similar to ubiquinone, can reduce myocardial hypertrophy and also decrease markers of oxidative stress in FRDA patients. Nevertheless, FRDA remains actually a severe neurodegenerative disease without any efficient therapy.

We have developed conditional mouse models that faithfully reproduce the biochemical and pathophysiological features of the human disease (cardiac Frda/MCK and neuronal Frda/PrP mutants) (41, 42). These animals show cardiodegeneration, dysfunction of large sensory neurons, deficiency of respiratory chain complexes I-III and aconitases, and mitochondrial iron accumulation. Iron accumulation occurs after the onset of pathology and more importantly late after inactivation of the Fe-S containing enzymes. We have recently reported that idebenone has a significant effect on the cardiac function and the life-span of the cardiac mouse model, despite the absence of measurable oxidative stress concomitant to mitochondrial iron accumulation (43). We now report further evidences by different complementary approaches that oxidative stress is, if present, a minor component in the murine pathophysiology. We also show that the cytosolic IRP1 is deprived of its ISC despite

the absence of oxidative stress, demonstrating for the first time that like the yeast ISC assembly machinery, the mammalian mitochondrial machinery is essential for cytosolic ISC biosynthesis. Finally, we have identified several deregulated genes in the FRDA murine cardiomyopathy through micro array analysis pointing to new pathways.

RESULTS

MnSOD mimetic therapy or Cu,ZnSOD overexpression has no beneficial effect on the murine FRDA cardiomyopathy

As frataxin-deficient cells and mice have been reported to present a lack of induction of the SODs, we tested the potential therapeutic effect of 5,10, 15, 20-tetrakis (4benzoic acid) porphyrin (MnTBAP) and Cu,ZnSOD overexpression on the murine FRDA cardiomyopathy (Frda/MCK), respectively. MnTBAP is a synthetic MnSOD (SOD2) mimetic which can substitute for the native antioxidant enzymes both *in vitro* and *in vivo* (44-48). The MnTBAP batch used had 56 U/mg SOD activity, and was shown to be protective in *in vitro* cell culture studies (49). MnTBAP was administered daily by intraperitoneal injection at the dose of 10 mg/kg/day from 3 weeks until death. No difference in body weight was seen between the two groups at any time during the study (data not shown). Kaplan-Meier survival curve showed that there was only a modest, non-significant difference between the two groups with a median survival time of 71 days (MnTBAP-treated Frda/MCK mutants, n=23) versus 68 (Placebo-treated littermates mutants, n=17) (Mantel-Cox Logrank p=0.099) (Figure 1A). The average survival of MnTBAP-treated animals was 74±9 days versus 69±9.4 days for placebo-treated animals (T-test p=0.038). Histological analyses showed no difference between the two groups (data not shown). Therefore, MnTBAP does not show positive pharmacological effect on the murine FRDA cardiomyopathy, at a dose, which is twice the dose known to rescue the cardiomyopathy associated with the MnSod nullizygous mice (5, 50, 51).

To test the potential effect of overexpression of the human cytosolic superoxide dismutase (Cu,ZnSOD; SOD1), we bred mice homozygous for the conditional frataxin allele carrying the tgN(SOD1)3Cje transgene (Frda L3/L3; Sod1+) with mice heterozygous for the deletion of frataxin exon 4 (Frda +/L-) carrying the MCK-Cre (tg/0) transgene, to obtain Frda L3/L-; MCK-Cre+; Sod1+ animals (SOD1+ overexpressing mutant animals). The SOD1 transgene was shown to express Cu,ZnSOD at approximately 2-5 fold the level of endogenous mouse Cu,ZnSOD in the heart, muscle, spinal cord and brain (data not shown) (52). As Frda L3/L-; MCK-Cre+ animals show over 99% frataxin deletion in the heart and skeletal muscle (41), the SOD1+ overexpressing mutant animals express human Cu,ZnSOD in the muscle cells deleted for frataxin which exhibit the phenotype. Kaplan-Meier survival curve showed no significant difference between the two groups (median survival rate of 72 and 73 for the SOD1+ overexpressing and the non-overexpressing mutant mice, respectively; Mantel-Cox Logrank p=0.45) (Figure 1B). The average survival of Cu,ZnSOD overexpressing mutant

animals was 75±10 days (n=22) versus mutant littermates at 74±9 days (n=19) (T-test p=0.3). Western blot analysis showed equal over-expression of human Cu,ZnSOD in the heart at 3 weeks and 10 weeks of age (data not shown), demonstrating that the lack of rescue is not due to a loss of Cu,ZnSOD overexpression over time.

Together, these results suggest not only that increased superoxide production in the mitochondria and the cytosol does not play a central role in the pathophysiology of the murine FRDA cardiomyopathy, but also that increased antioxidant defense is not sufficient to attenuate the FRDA phenotype.

Absence of oxidative stress and decrease of superoxide dismutase expression in frataxin-deficient tissues

In order to correlate the absence of superoxide production in FRDA pathology with the antioxidant response, we followed the kinetics of the MnSod mRNA and protein levels in mouse tissues deficient for frataxin, particularly in the heart and cerebellum of Frda/MCK mutants and Frda/PrP mutants, respectively. As expected, MnSod mRNA expression level increased with age (2-10 weeks) in the heart of control mice (Figure 2A). Similarly, the MnSod mRNA expression level increased between 2 to 7 weeks of age in the heart of Frda/MCK mutant mice. However, it dramatically decreased from 7 to 10 weeks (35±7% compared to control littermates at 8 weeks of age) (Figure 2A). Western blot analysis showed a 53±19% decrease in MnSod protein expression at 10 weeks in the Frda/MCK mutants (p=0.04, Figure 2A) thereby confirming transcriptional data. These data are in agreement with the previously reported absence of MnSod activity at 7-10 weeks (23). This lack of activity appears to be a secondary shut down rather than a lack of induction. It is important to note that at 7 weeks of age, the respiratory chain enzyme activities are extremely decreased with 20% residual activity, and that mitochondrial iron accumulation although not statistically significant, is clearly visible as scattered intramitochondrial iron deposits (41, 43).

In the cerebellum of the Frda/PrP neurological mouse model, we observed a significant and progressive decrease both in the MnSod transcript and protein expression (Figure 2B), although not as severe as in the heart model, probably due to the presence of non-neuronal and non-deleted tissues. The protein decrease was delayed with respect to the corresponding mRNA decrease. By 40 weeks of age, when all frataxin-deleted cells had died (as demonstrated by the normalization of frataxin levels (Figure 2C)), relative MnSod mRNA and protein level went back to wild type level (Figure 2B). Therefore, similarly to the frataxin-deficient heart, the frataxin deficient cerebellum has a lower MnSod expression level.

In order to test whether reduced MnSod and Cu,ZnSod expression is a cause or a consequence of the pathology, we tested for the presence (cause) or absence (consequence) of oxidative stress markers. We previously reported a clear and significant decrease in oxidized proteins and an absence of lipoperoxide increase in the heart of Frda/MCK animals from 7 weeks onwards (43). Oxidized protein level was determined in the cerebellum of the neuronal mouse model (Frda/PrP). Again no significant increase in oxidized proteins was observed at any age between the mutant animals and the control littermates (Figure 2D). There was a slight decrease in oxidized protein at 40 weeks of age, although the significance is unknown. These results reveal that complete frataxin deficiency does not induce a measurable oxidative stress even in a neuronal tissue over a longer period of time. The MnSod expression and activity is not induced at a higher level in the mutant animals early in the pathology compared to wild-type animals, while it is even decreased at late stages, although there is an elevated mitochondrial iron accumulation. Altogether, these results suggest that, contrary to widely discussed hypotheses, complete frataxin deficiency induces a drop of free radical production, presumably as a consequence of reduced mitochondrial activity, and further suggest that the mitochondrial iron accumulation does not generate $OH^{\bullet}$ through Fenton reaction.

Cytosolic aconitase activity and iron homeostasis regulation in frataxin-deficient tissues

We have previously reported an overall reduction of mitochondrial ISC enzyme activities in the heart of Frda/MCK mutant mice, which occurred before intramitochondrial iron accumulation (41). In the cytosolic compartment of mammalian cells, the bi-functional Iron Regulatory Protein-1 (IRP-1) participates in maintaining intracellular iron homeostasis at a post-transcriptional level (53). It has been well described that under iron depletion, IRP-1 devoid of its ISC, binds specific Iron Responsive Elements (IRE) located on ferritin and transferrin receptor mRNAs. IRP-1/IRE interactions inhibit translation of ferritin (involved in iron storage) and stabilize the transferrin receptor mRNA (involved in iron import). Once intracellular iron pool is restored, IRP-1 no longer binds the IRE sequences and becomes an aconitase through assembly/insertion of its [4Fe-4S] cluster. As a result, ferritin mRNA is translated and transferrin receptor mRNA is degraded. We investigated the fate of cytosolic aconitase/IRP-1 activities in the Frda/MCK model compared to wild type mice, at 5, 8 and 10 weeks of age. Cytosolic aconitase activity of IRP-1 progressively decreased by 20, 50 and 80 % with age in the heart of MCK mutant as compared to that of wild type mice (Figure 3A). Interestingly, this aconitase activity loss was accompanied by gradual increase in IRP-1/IRE binding activity, however reaching only 37 % of its full binding activity at 10 weeks of age

(Figure 3B-C). In wild type animals, IRP-1 displayed no activation of IRE binding activity from 5 to 10 weeks and was prominently converted to aconitase activity (Figure 3). Activation of IRP-1 in Frda/MCK mice from the age of 5 weeks indicates that IRP-1 is deprived of its ISC. This ISC deficit in cytosol in absence of frataxin points to the important role of the mitochondrion in the cytosolic ISC biogenesis. Furthermore, the activation of IRP-1 from week 5 to week 10 could explain later iron accumulation observed in mitochondria. In the heart of both wild type and mutant mice, we were unable to detect IRE binding activity by IRP2, which is however not an ISC regulated iron responsive protein (data not shown).

Since injury of iron-containing membrane proteins (e.g. ISC proteins and/or hemoproteins) might increase the demand for cell iron import, we investigated the effect of frataxin deficiency on the expression level of genes involved in iron metabolism over the evolution of the disease in the heart of Frda/MCK mutants. In the early stage of the cardiac disease (2-5 weeks), there was no significant difference in the expression of any of the iron metabolism related genes (IRP1, IRP2, transferrin receptor, ferritin light and heavy chains) (Figure 4). By 10 weeks of age, a late stage of the disease with intramitochondrial iron accumulation, RT-PCR analysis showed down-regulation in both aconitase/IRP1 and the transferrin receptor (59±10 % ($p=0.006$) and 46±9 % ($p=0.05$), respectively), while the expression of the ferritin light chain was up regulated by 266±29 % ($p=0.0001$) (Figure 4A). Interestingly, the expression level of the ferritin light chain is already increased at 5 weeks of age ($p=0.003$) suggesting that iron overload is already detected prior to iron accumulation. Western blot analyses show no difference in ferritin L expression from 2-5 weeks, while there is an increase at 10 weeks (Figure 4B). Similarly, western blot analysis shows a clear decrease in the transferrin receptor at 10 weeks (45% wild type expression; data not shown). These data indicate that, despite IRP1 activation, iron homeostasis regulatory mechanisms in frataxin-deficient cardiac cells anticipate the mitochondrial iron accumulation by increasing its storage capacity (ferritin L) and simultaneously decreasing its import system (transferrin receptor). Interestingly, ferritin H is not deregulated, further confirming that the observed regulation is IRP1 independent. The two genes have been shown to be differentially regulated at the transcriptional level for example during inflammation (ferritin H) or hypoxic conditions (ferritin L) (54). The inefficacy of IRP1 activation concomitant to its mRNA down-regulation suggests that the cell has a mean of regulating the iron import when ISC are deficient. Therefore, although the mitochondrial iron accumulation does not induce oxidative stress, the iron overload appears visible to the cell.

We show that cytosolic aconitase activity progressively decreases with age in frataxin-deficient mouse tissues, accompanied by a partial gradual increase in IRP1/IRE binding activity, indicating that IRP1 is deprived of its ISC despite the absence of oxidative stress. These data demonstrate for the first time in a mammalian system that the mitochondrial ISC assembly machinery is essential for cytosolic ISC biogenesis, similarly to the evolutionary conserved yeast machinery.

Pathways deregulated in Frda/MCK animals

To identify deregulated genes in frataxin-deficient cardiomyocytes, we performed microarray analysis of mouse heart RNA using the 'Mitochip' (MAMMAG, University of California, Irvine). The Mitochip is a specialized mouse custom cDNA micro array targeted towards the study of mitochondrial bioenergetics encompassing 850 individual genes. The cDNA clones were selected based on a survey of the literature for all mammalian genes known to function in relation to the mitochondria (mitochondrial bioenergetics, metabolism, reactive oxygen species, and apoptosis). These include genes identified from functional genomic data and genome-wide orthology searches between yeast and humans for nDNA mitochondria-related genes. These clones were ordered from the NIA sequence-verified mouse cDNA clone collection, while the mtDNA sequences were amplified by direct, gene-specific amplification. A list of the genes that are on the chip is available online as a supplement (Table 2, supplemental data).

Differential expression was analyzed between frataxin-deficient and wild type littermate mice. We decided to assess gene expression in heart of 5 weeks old mice, at a stage of early cardiac pathology before massive cardiac remodeling, post-necrotic fibrosis, and iron accumulation. The significantly altered genes are listed in Table 1. Only 30 out of the 850 transcripts present on the mitochip show significant alterations (20 up-regulated, and 10 down-regulated) (Table 1). Gene products of altered transcripts function in various biochemical pathways, including sulfur amino acid synthesis, mitochondrial respiratory chain, response to cardiac hypertrophy and damage. Of interest, major genes involved in oxidative stress response such as superoxide dismutases, glutathione peroxidases, and catalases were not up regulated in the heart of 5 weeks old mutant animals.

To confirm the microarray results, we used quantitative real-time RT-PCR analysis to investigate the RNA expression of 8 up-regulated genes in the heart of MCK mutants and control littermate mice at the three stages of the murine FRDA cardiomyopathy progression (3, 5, and 10 weeks). The real-time RT-PCR data at 5 weeks of age agreed with our original

cDNA micro array results (Figure 5 and Table 1), independently validating the conclusions drawn from our micro array analysis. The genes that are up-regulated can be classified into three groups according to their expression pattern: the genes that are highly up-regulated (3-4 fold at 3 weeks and 20-30 fold at 5 weeks) early in the pathology (methylenetetrahydrofolate dehydrogenase (NAD+ dependent) and cyclohydrolase (Mthfd2) and asparagine synthetase (Asn)), the genes that are moderately up-regulated early in the pathology (asparaginyl- and glutamyl-tRNA synthetase (NARS and GluRS)) and the genes that are moderately up-regulated at an intermediate stage (Glutathione S-transferase omega 1 (Gsttl), Cathepsin L (Ctsl), Ferritin L (Ftl), and vacuolar ATPase H) (Figure 5). As Mthfd2 and Asn were already up regulated at 3 weeks, we also looked at their expression pattern at 2 weeks of age, prior to any detectable biochemical (i.e. ISC enzyme deficit) and functional phenotype. We found that Mthfd2 is already up regulated by 1,5 fold at 2 weeks of age in the heart of the Frda/MCK mutants ($p=0.01$) compared to wild type littermates (Figure 5). Mthfd2 is therefore the first pathological mitochondrial marker of frataxin deficiency in these animals (there is no detectable frataxin mRNA nor protein at 2 weeks of age, data not shown). We note that expression of several genes involved in intracellular metabolism of amino acids were impaired in frataxin deficient heart tissue. These include Mthfd2, asparagine synthetase, and Gln-, Asn-, and Ala-tRNA synthetase.

DISCUSSION

Since the absence of frataxin leads to a mitochondrial respiratory chain dysfunction followed by mitochondrial iron accumulation, it has been postulated on many occasions that oxidative stress generated through the defective respiratory chain and Fenton's reaction is at the center of the FRDA disease further aggravating the primary ISC deficit. Several attempts using antioxidants have been realized to find an efficient therapy for FRDA. Idebenone, a short chain analog of Coenzyme Q10 has shown a positive impact on the cardiac hypertrophy in a majority of patients including in short treatment periods, although its efficacy on the neurological condition is unknown (36-40). A combined therapy involving long term treatment with high doses of vitamin E and coenzyme Q10 has shown rapid and sustained increase in the energy generated by the heart and skeletal muscle, however accompanied only by a partial improvement of the symptoms (55). Clearly, more effective drug treatments are needed. We have previously shown that idebenone had a significant and clear cardioprotective effect on the murine FRDA cardiomyopathy by delaying the onset and the progression of the disease, thereby increasing the life span of the animals (43).

In the present paper, we showed that MnTBAP, a well-known mitochondrial antioxidant, has no effect on the survival rate of the animals. MnTBAP is a low molecular weight salen-manganese complex with antioxidant catalytic activities (EUK compounds) shown to catalytically scavenge the reactive oxygen species superoxide, hydrogen peroxide as well as reactive nitrogen species, all potential contributors to neurological and cardiac injury in circumstances of oxidative stress (56). *In vivo* studies demonstrated that administration of EUK compounds significantly prolongs survival and reduces oxidative stress in a mouse model of Amyotrophic Lateral Sclerosis (57), prevents neuronal death and reduces oxidative damage following kainic acid induced seizures in rats (56), and extends lifespan in the nematode (58). MnTBAP (or modified MnTBAP capable of passing the blood-brain barrier) is able to rescue the cardiomyopathy and partially rescue the pronounced neurological phenotype of MnSod nullizygous mice in a dose-dependent manner by protecting the cells from superoxide insult (in particular, the catalytic activities of complexes I, II, III and IV, known to be highly sensitive to superoxide-mediated inactivation, are restored to wild type levels) (59, 60). Collectively, these different studies illustrate the utility of this class of antioxidants in preventing damage associated with oxidative stress. We have shown here that MnTBAP, unlike idebenone, is unable to protect the cardiomyopathy of frataxin-deficient mice, suggesting that free radicals production in murine FRDA model is a minor component

in the pathophysiology. Similarly, overexpression of cytosolic Cu,ZnSOD in the cardiac frataxin-deficient mice is ineffective although it has been shown to protect mice from cerebral and intestinal ischemia-reperfusion injury and from pulmonary oxygen toxicity, therefore also excluding a role of cytosolic free radicals. By contrast, it has been also described that high Cu,ZnSOD expression level in transgenic mice has been linked to increased rates of lipid peroxidation, increased levels of protein carbonyls, and hypersensitivity to oxidative stress (61-63). In conclusion, as cytosolic overexpression of Cu,ZnSOD in our frataxin-deficient mice does not induce neither positive nor negative changes, an impairment in oxidative stress defense and a primary role of oxidative stress in the murine cardiac FRDA pathophysiology are both very unlikely.

We have also demonstrated that frataxin deficient tissues behave as if they were less challenged by free radicals. In agreement with our previous results on the cardiac model, we demonstrate the absence of increased oxidative stress markers (protein carbonylation (this manuscript and (43)) and lipid peroxidation (43)) in the neuronal model. In addition, no significant difference of MnSod expression in tissues deleted for frataxin (both cardiac and neuronal) was found in the early step of the pathology, while a significant reduction was observed late in the disease, when the respiratory chain activity is strongly diminished (illustrated in cardiac tissues by reduced complexe I, II and III activities) (41, 43). This decrease in MnSod transcript and protein correlates with the decrease in activity previously measured (41). These data therefore suggest that the previously observed lack of SODs induction following exogenous free radical insults on FRDA patient fibroblasts (23, 35) is most likely an indication of reduced endogenous superoxide production, rather than a source of free radical injury, as generally assumed. The absence of changes in ferritin H expression further suggests a lack of oxidative insult, as this gene is extremely sensitive to oxidative stress (64, 65). Taken together, these results clearly demonstrate that oxidative stress, whether mediated by iron or by mitochondrial dysfunction, is not a primary pathological component of the disease in the mouse models. Our results rather indicate that while frataxin deficient cardiomyocytes are perfectly able to induce normal MnSOD response at the early step of pathology, they fail to do so when mitochondrial iron accumulates, demonstrating that superoxides in the late events of the disease do not challenge them. This suggests that iron might be coupled to a protein complex in the mitochondria, preventing it from reacting through Fenton reaction.

Although our results appear at first to be in contradiction with the general agreement, evidences of oxidative damage in FRDA patients were contradictory. While brain tissues from

FRDA patients failed to reveal any changes in MDA levels (66), plasma MDA level (25, 34), and urine 8-hydroxy-2'-deoxyguanosine levels (24) were increased, indicating increased oxidative damage. In one report, the severity of lipid peroxidation correlated with length of disease duration as well as clinical severity (34). This is consistent with oxidative damage increasing as the disease advances possibly as a late consequence of chronic illness. Therefore, the observations of increased oxidative damage markers should not be taken as proof of primary involvement of oxidative stress in FRDA patients.

The decrease in SODs at late stages in the mutant animals could be in part attributed to the decrease in oxidative phosphorylation. This hypothesis is supported by genetic screens in *Saccharomyces cerevisiae* which identified mitochondrial proteins involved in the assembly/maturation of ISC (*Ssq1*, *Jac1*, *Nfs1*, and *Isu1*) as suppressors of endogenous sources of oxidative stress (*seo* mutants), in fact suppressors of the phenotype caused by the *Cu,ZnSod* disruption. *Seo* mutants in the absence of *Cu,ZnSod* mutation (normal antioxidant defense) result in impairment of respiration and reduction in activities of the mitochondrial ISC-containing enzymes, aconitase and succinate dehydrogenase (as in FRDA patients' cardiomyocytes and in our frataxin-deficient mouse models. Moreover, *seo* mutants do not show general antioxidant behavior, fail to reduce sensitivity to environmental oxidants (67), and over-accumulate mitochondrial iron which is not EPR-detectable "free" iron (68). The pool of iron that is detectable by EPR spectroscopy increases when superoxide levels are elevated. This data suggests, as observed in Δ*Yfh1* frataxin deficient yeast, that mitochondrial iron accumulation is non-toxic in "non-oxidative" conditions.

Finally, micro array analysis revealed no significant transcriptional alteration in any of the major oxidative stress response pathways or in iron homeostasis, early in the disease (in agreement with transcriptional data obtained from FRDA patient cell lines (69)). In contrast, Mthfd2 mRNA was increased in the frataxin-deficient heart tissues at 2 weeks prior to any biochemical or clinical phenotype, making it the first molecular mitochondrial marker of the disease in the mouse. MTHFD2 is a bifunctional enzyme, which catalyses the reversible conversion of 10-formyltetrahydrofolate (10-formylTHF) to 5,10-methenylTHF, and of 5,10-methenylTHF to 5,10-methyleneTHF. Normal tissues contain low levels of this mRNA, with the exception of thymus and testis. The activation of this enzyme may represent an attempt to restore folate intermediates for DNA synthesis and methylation, or may be indirectly related to the deregulated sulfur amino acid metabolism (69). The expression of these genes is directly under the control of the transcription factor Atf4 as a response to either amino acid (amino acid response) or glucose (ER stress response) deprivation. No increase in Atf4

mRNA expression was found until 10 weeks of age (data not shown), but induced Atf4 expression occurs predominantly via translation control (70, 71). Therefore, early Mthfd2 overexpression may represent a new altered pathway in FRDA.

Using FRDA mouse models, we have shown that oxidative stress seems to play a minor role in the FRDA pathophysiology. Nevertheless, we have previously shown that idebenone has a significant and clear protective effect on the survival and on the cardiac function, as it delays the onset and disease progression. In contrast, MnTBAP, a well-known effective mitochondrial antioxidant has no effect. These observations raise important questions regarding the therapeutic approaches and the mechanism of action of antioxidants such as idebenone. Idebenone action as electron donor in the respiratory chain might be more effective in the FRDA-deficient cells, as it may bypass coenzyme Q10 which is less solicited by the defective complexes I and II. Although our data do not resolve the issue as to the mechanism by which antioxidants such as idebenone act, they clearly show that oxidative stress is not primary consequence of frataxin deficiency and iron accumulation in FRDA. Therefore, therapeutic approaches for FRDA should not be limited to antioxidant and iron chelators but should target direct frataxin partners within the mitochondria. Finally, the concept of FRDA as a paradigm for neurodegenerative diseases due to oxidative stress should be revised.

MATERIALS AND METHODS

All methods employed in this work are in accordance with the *Guide for the Care and Use of Laboratory Animals* published by the US National Institutes of Health (NIH Publications No. 85-23, revised 1996).

Micro array Analysis

MITOCHIP Micro array Construction – A total of 850 sequence verified cloned mouse cDNAs/genes were selected from NIA clone set, based on their relevance to mitochondrial function, reactive oxygen species biology, and apoptosis (Supplemental material). The 15 mtDNA transcripts (rRNAs 12S and 16S and 13 mRNAs) were included after PCR amplification from mouse mtDNA templates. Clone inserts were amplified from bacterial clones in 96-well format. Modified M13 PCR primers (5'-tgtaaaacgacggccagt -3' forward, 5'-caggaaacagctatgacc-3' reverse) were used in standard 100 □l PCR (72). The quantity and integrity of the amplification products were verified by gel electrophoresis and purified over 96-well multiscreen PCR plates following the manufacturer's recommendations (Millipore, Bedford, MA) adjusted to150 ng/□l in 50% DMSO and spotted onto poly-L-lysine coated glass slides using a GMS 417 (Genetics Microsystems, Inc). DNAs were crosslinked to the slides using 80 mjoules of ultraviolet energy (Stratagene Stratalinker, La Jolla, CA), baked for two hours at 70°C and stored under low humidity.

RNA Labeling and MitoChip Hybridization – Total RNA was isolated from 3 wild type and 3 Frda/MCK heart tissue 5 weeks old mice using Trizol reagent following the manufacturer protocol (Invitrogen, Carlsbad, CA) and mutant and wild type total RNAs were pooled separately. Hybridization cDNA probes were prepared from 40 □g of DNAse-treated total pooled RNA from mutant and wild type with SuperScript II RNaseH reverse transcriptase (Invitrogen, Carlsbad, CA) in the presence of fluorescent nucleotides Cy3- or Cy5-dCTP (Amersham Pharmacia Biotech) during 2 hours at 42°C. Template RNA was degraded with 50 mM NaOH at 70°C for 10 min, and then neutralized with 50 mM HCl and the cDNAs were purified using Qiagen PCR cleanup kit (PCR Cleanup kit, Qiagen, Valencia, CA) and quantified on a spectrophotometer using the specific wavelength for each dye to compensate for differences in the labeling and chemical properties of the Cy3 (549 nm) and Cy5 (650 nm) dyes. Twenty-five picomoles of each probe were mixed and dried and the probe was resuspended in the following buffer formamide 25%, 20SSC 5x, SDS 0.1%, in a 22 □l final

volume. Blocking agents were added to the hybridization buffer at a final concentration of 0.5 mg/ml of yeast tRNA, 0.5 mg/ml of polyA RNA and 0.05 mg/ml of Cot-1 DNA. The Cy3-Cy5 labeled cDNA probes were denatured at 95°C for two minutes, spred over the cDNA array, and the slides incubated in a hybridization chamber (Corning, Acton, MA) at 45°C for 16 hours. After hybridization, the slides were washed in 1x SSC/0.1% SDS for 5 min at 45°C followed by one wash in 1x SSC/0.1% SDS and 0.1x SSC/0.1% SDS for 5 min each at room temperature. The arrays were dried by centrifugation at 50 g for 5 minutes and scanned immediately.

Micro array Data Analysis – The intensities of the spots were analyzed by using a scanner (Affymetrix 428 array scanner) for both red and green channels simultaneously. Fluorescence intensity was measured for each chip and normalized to the average fluorescence intensity for the entire chip and all scanned arrays were saved as 16-bit TIFF images files and analyzed using Imagene software (Biodiscovery, Los Angeles, USA). The results from the seven independent arrays were combined for statistical analysis, and lowess normalization utilized for all samples. Spots were selected with at least a signal to background ratio were two or more.

MnTBAP treatment – For animal studies, MnTBAP was dissolved in sterile water at 5mg/ml. MnTBAP was prepared and injected as described previously (58). Mice were genotyped as described previously (41) and then injected intraperitoneally on a daily basis at 5 mg/kg body weight from 3 weeks of age until death.

Genotyping and DNA analysis – Genotyping and DNA analysis were performed as previously described (41). To test the potential effect of overexpression of the human cytosolic superoxide dismutase (Cu,ZnSOD; SOD1), we bred mice homozygous for the conditional frataxin allele carrying the tgN(SOD1)3Cje transgene (Frda L3/L3; Sod1+) (52) with mice heterozygous for the deletion of frataxin exon 4 (Frda +/L-] carrying the MCK-Cre (tg/0) transgene, to obtain Frda L3/L-; MCK-Cre+; Sod1+ animals (SOD1+ overexpressing mutant animals).

Quantitative RT-PCR (Q-RT-PCR) – Total RNA extractions from tissues were performed using Trizol reagents (Invitrogen), according to the manufacturer's recommendations. RT-PCR analysis was performed as described by the kit manufacturer (Promega). DNAseI-treated total RNA were reverse transcribed with Moloney murine leukemia virus reverse transcriptase

(MMLV-RT, Promega) and random hexamer (0.1 □M) and oligo(dT) (0.1 □M). The transcripts were quantified on a real-time thermal cycler (LightCycler, Roche Diagnostics). Total RNAs were extracted from cell and treated with RNAse-free DNAseI. The RNAs (1 □g) were converted to cDNAs with random hexamer (0.1 □M) and oligo(dT) primer (0.1 □M) and MMLV-RT (Promega) in 50□l reaction volume, and the reaction was diluted with Milli-Q water (80 □l). Hprt transcripts were chosen as a reference gene, and serial dilution of RT were used for standards for each couple of primers. Q-RT-PCR was carried out in 10 □l reaction volume containing 2 □l of template cDNAs, 1X FastStart DNA Master SYBR Green I buffer (Roche), 3 mM $MgCl_2$, and 0.3 □M each primer. PCR conditions were 95°C for 5 min; 60°C, 20 sec; 72°C, 20 sec; 40-50 cycles. After PCR, absence of unwanted by-products was confirmed by automated melting curve analysis. The molar amounts of Frda and Hprt transcripts were calculated based on the crossing point analysis, with standard curves generated from the standard cDNAs. Frda transcript levels were normalized with Hprt transcripts levels in the same samples.

Immunoblot analysis **–** Immunoblot were performed as previously described (41). Anti-ferritin antisera was kindly provided by Dr. J. Brock, Glasgow University (Glasgow, UK) and mouse monolonal anti-vinculin antibody was used according to manufacturers protocol (Sigma).

Detection of Carbonylated Proteins ("OxyBlot") **–** Carbonylated proteins were detected using the Oxyblot Oxidation Protein Detection Kit (Intergen, Temecula). 10-30 □g of protein were reacted with 2,4-dinitrophenylhydrazine for 15 min at 25°C. Samples were resolved on 12% denaturing polyacrylamide gels, and 2,4-dinitro-phenol-derivatized proteins were identified by immunoblot assays using an anti-2,4-dinitrophenol antibody. To monitor sample loading, the β̃tubulin was also detected by immunostaining with the corresponding antibody.

IRP1/Aconitase Activity

Preparation of cytosolic fractions **–** By using a glass homogenizer (Duall 21), tissues were disrupted in 500 □l of 0.25 M sucrose, 100 mM HEPES, pH7.4 at 4°C. The resulting suspension was centrifuged at 230 g for 10 min at 4°C and after red blood cell lysis, the white pellet was resuspended in 0.25 M sucrose, 100 mM HEPES, pH7.4 and treated with 0.01% digitonin for 10 min at 4°C to lyse cells without damaging mitochondria. The lysate was then

centrifuged at 100 000 g for 1 h at 4°C to spin down any particle material. Cytosolic extract was tested for aconitase activity and then stored at –80°C until use.

Gel Mobility shift assay **–** IRP/IRE interactions were measured by incubating a molar excess of (^{32}P)CTP-labeled IRE transcript with 2-5 □□ of cytosolic extracts in a 20 □l reaction volume. After 10 min incubation at room temperature, one unit of RNAse T1 and 5 mg/ml heparin were sequentially added for 10 min each. IRP/IRE complexes were run on a non-denaturing 6% polyacrylamide gel. In parallel experiments, samples were routinely treated with 2% 2-Mercaptoethanol (2-ME) prior to addition of the IRE probe to allow full expression of IRE binding activity.

Determination of aconitase activity **–** Aconitase activity was measured spectrophotometrically by following the disappearance of *cis*-aconitate at 240 nm. The reaction volume (600 □l) contains 30 □□ of cytosolic extract in 100 mM Tris-HCl, pH7.4, and kinetic was started by the addition of 15 □l of 20 mM cis –aconitate. Units represent nanomoles of substrate consumed/min at 37°C (□=3,4 mM^{-1} cm^{-1}).

ACKNOWLEDGEMENTS

We thank J.L. Mandel and members of his laboratory for discussions and comments; N. Lagarde and B. Guillon for technical support; R. Kahn for the MCK-Cre Transgenic animals. This work was supported by funds from the European Community (contract QLRT-CT-1999-00584), the Muscular Dystrophy Association of America (MDA), National Ataxia Foundation (NAF), INSERM and CNRS. H.S was supported by the Association Française contre l'ataxie de Friedreich (AFAF), the Association "Connaître les Syndomes Cérébélleux" (CSC) and the European Community (EC).

REFERENCES

1. Beal, M.F. (1997) Oxidative damage in Neurodegenerative diseases. *The neuroscientist,* **3,** 21-27.

2. Langley, B. and Ratan, R.R. (2004) Oxidative stress-induced death in the nervous system: cell cycle dependent or independent? *J. Neurosci. Res.,* **77,** 621-629.

3. Chance, B., Sies, H. and Boveris, A. (1979) Hydroperoxide metabolism in mammalian organs. *Physiol. Rev.,* **59,** 527-605.

4. Lass, A., Agarwal, S. and Sohal, R.S. (1997) Mitochondrial ubiquinone homologues, superoxide radical generation, and longevity in different mammalian species. *J. Biol. Chem.,* **272,** 19199-19204.

5. Melov, S., Schneider, J.A., Day, B.J., Hinerfeld, D., Coskun, P., Mirra, S.S., Crapo, J.D. and Wallace, D.C. (1998) A novel neurological phenotype in mice lacking mitochondrial manganese superoxide dismutase. *Nat. Genet.,* **18,** 159-163.

6. Lebovitz, R.M., Zhang, H., Vogel, H., Cartwright, J., Jr., Dionne, L., Lu, N., Huang, S. and Matzuk, M.M. (1996) Neurodegeneration, myocardial injury, and perinatal death in mitochondrial superoxide dismutase-deficient mice. *Proc. Natl. Acad. Sci. U S A,* **93,** 9782-9787.

7. Stohs, S.J. and Bagchi, D. (1995) Oxidative mechanisms in the toxicity of metal ions. *Free Radic. Biol. Med.,* **18,** 321-336.

8. Cafe, C., Torri, C., Bertorelli, L., Tartara, F., Tancioni, F., Gaetani, P., Rodriguez y Baena, R. and Marzatico, F. (1995) Oxidative events in neuronal and glial cell-enriched fractions of rat cerebral cortex. *Free Radic. Biol. Med.,* **19,** 853-857.

9. Kish, S.J., Bergeron, C., Rajput, A., Dozic, S., Mastrogiacomo, F., Chang, L.J., Wilson, J.M., DiStefano, L.M. and Nobrega, J.N. (1992) Brain cytochrome oxidase in Alzheimer's disease. *J. Neurochem.,* **59,** 776-779.

10. Mutisya, E.M., Bowling, A.C. and Beal, M.F. (1994) Cortical cytochrome oxidase activity is reduced in Alzheimer's disease. *J. Neurochem.,* **63,** 2179-2184.

11. Swerdlow, R.H., Parks, J.K., Miller, S.W., Tuttle, J.B., Trimmer, P.A., Sheehan, J.P., Bennett, J.P., Jr., Davis, R.E. and Parker, W.D., Jr. (1996) Origin and functional consequences of the complex I defect in Parkinson's disease. *Ann. Neurol.,* **40,** 663-671.

12. Brown, R.H., Jr. (1997) Amyotrophic lateral sclerosis. Insights from genetics. *Arch. Neurol.,* **54,** 1246-1250.

13. Koutnikova, H., Campuzano, V., Foury, F., Dolle, P., Cazzalini, O. and Koenig, M. (1997) Studies of human, mouse and yeast homologues indicate a mitochondrial function for frataxin. *Nat. Genet.,* **16,** 345-351.
14. Priller, J., Scherzer, C.R., Faber, P.W., MacDonald, M.E. and Young, A.B. (1997) Frataxin gene of Friedreich's ataxia is targeted to mitochondria. *Ann. Neurol.,* **42,** 265-269.
15. Rotig, A., de Lonlay, P., Chretien, D., Foury, F., Koenig, M., Sidi, D., Munnich, A. and Rustin, P. (1997) Aconitase and mitochondrial iron-sulphur protein deficiency in Friedreich ataxia. *Nat. Genet.,* **17,** 215-217.
16. Harding, A.E. (1981) Friedreich's ataxia: a clinical and genetic study of 90 families with an analysis of early diagnostic criteria and intrafamilial clustering of clinical features. *Brain,* **104,** 589-620.
17. Campuzano, V., Montermini, L., Lutz, Y., Cova, L., Hindelang, C., Jiralerspong, S., Trottier, Y., Kish, S.J., Faucheux, B., Trouillas, P. *et al.* (1997) Frataxin is reduced in Friedreich ataxia patients and is associated with mitochondrial membranes. *Hum. Mol. Genet.,* **6,** 1771-1780.
18. Foury, F. (1999) Low iron concentration and aconitase deficiency in a yeast frataxin homologue deficient strain. *FEBS Lett.,* **456,** 281-284.
19. Waldvogel, D., van Gelderen, P. and Hallett, M. (1999) Increased iron in the dentate nucleus of patients with Friedrich's ataxia. *Ann. Neurol.,* **46,** 123-125.
20. Babcock, M., de Silva, D., Oaks, R., Davis-Kaplan, S., Jiralerspong, S., Montermini, L., Pandolfo, M. and Kaplan, J. (1997) Regulation of mitochondrial iron accumulation by Yfh1p, a putative homolog of frataxin. *Science,* **276,** 1709-1712.
21. Foury, F. and Cazzalini, O. (1997) Deletion of the yeast homologue of the human gene associated with Friedreich's ataxia elicits iron accumulation in mitochondria. *FEBS Lett.,* **411,** 373-377.
22. Lamarche, J.B., Cote, M. and Lemieux, B. (1980) The cardiomyopathy of Friedreich's ataxia morphological observations in 3 cases. *Can. J. Neurol. Sci.,* **7,** 389-396.
23. Chantrel-Groussard, K., Geromel, V., Puccio, H., Koenig, M., Munnich, A., Rotig, A. and Rustin, P. (2001) Disabled early recruitment of antioxidant defenses in Friedreich's ataxia. *Hum. Mol. Genet.,* **10,** 2061-2067.
24. Schulz, J.B., Dehmer, T., Schols, L., Mende, H., Hardt, C., Vorgerd, M., Burk, K., Matson, W., Dichgans, J., Beal, M.F. *et al.* (2000) Oxidative stress in patients with Friedreich ataxia. *Neurology,* **55,** 1719-1721.

25. Emond, M., Lepage, G., Vanasse, M. and Pandolfo, M. (2000) Increased levels of plasma malondialdehyde in Friedreich ataxia. *Neurology,* **55,** 1752-1753.
26. Muhlenhoff, U., Richhardt, N., Ristow, M., Kispal, G. and Lill, R. (2002) The yeast frataxin homolog Yfh1p plays a specific role in the maturation of cellular Fe/S proteins. *Hum. Mol. Genet.,* **11,** 2025-2036.
27. Muhlenhoff, U., Richhardt, N., Gerber, J. and Lill, R. (2002) Characterization of iron-sulfur protein assembly in isolated mitochondria. A requirement for ATP, NADH, and reduced iron. *J. Biol. Chem.,* **277,** 29810-29816.
28. Lesuisse, E., Santos, R., Matzanke, B.F., Knight, S.A., Camadro, J.M. and Dancis, A. (2003) Iron use for haeme synthesis is under control of the yeast frataxin homologue (Yfh1). *Hum. Mol. Genet.,* **12,** 879-889.
29. Huynen, M.A., Snel, B., Bork, P. and Gibson, T.J. (2001) The phylogenetic distribution of frataxin indicates a role in iron-sulfur cluster protein assembly. *Hum. Mol. Genet.,* **10,** 2463-2468.
30. Yoon, T. and Cowan, J.A. (2003) Iron-sulfur cluster biosynthesis. Characterization of frataxin as an iron donor for assembly of [2Fe-2S] clusters in ISU-type proteins. *J. Am. Chem. Soc.,* **125,** 6078-6084.
31. Yoon, T. and Cowan, J.A. (2004) Frataxin-mediated iron delivery to ferrochelatase in the final step of heme biosynthesis. *J. Biol. Chem.,* **279,** 25943-25946.
32. Bulteau, A.L., O'Neill, H.A., Kennedy, M.C., Ikeda-Saito, M., Isaya, G. and Szweda, L.I. (2004) Frataxin acts as an iron chaperone protein to modulate mitochondrial aconitase activity. *Science,* **305,** 242-245.
33. Wong, A., Yang, J., Cavadini, P., Gellera, C., Lonnerdal, B., Taroni, F. and Cortopassi, G. (1999) The Friedreich's ataxia mutation confers cellular sensitivity to oxidant stress which is rescued by chelators of iron and calcium and inhibitors of apoptosis. *Hum. Mol. Genet.,* **8,** 425-430.
34. Bradley, J.L., Homayoun, S., Hart, P.E., Schapira, A.H. and Cooper, J.M. (2004) Role of oxidative damage in Friedreich's ataxia. *Neurochem. Res.,* **29,** 561-567.
35. Jiralerspong, S., Ge, B., Hudson, T.J. and Pandolfo, M. (2001) Manganese superoxide dismutase induction by iron is impaired in Friedreich ataxia cells. *FEBS Lett.,* **509,** 101-105.
36. Rustin, P., von Kleist-Retzow, J.C., Chantrel-Groussard, K., Sidi, D., Munnich, A. and Rotig, A. (1999) Effect of idebenone on cardiomyopathy in Friedreich's ataxia: a preliminary study. *Lancet,* **354,** 477-479.

37. Hausse, A.O., Aggoun, Y., Bonnet, D., Sidi, D., Munnich, A., Rotig, A. and Rustin, P. (2002) Idebenone and reduced cardiac hypertrophy in Friedreich's ataxia. *Heart,* **87,** 346-349.
38. Artuch, R., Aracil, A., Mas, A., Colome, C., Rissech, M., Monros, E. and Pineda, M. (2002) Friedreich's ataxia: idebenone treatment in early stage patients. *Neuropediatrics,* **33,** 190-193.
39. Schols, L., Vorgerd, M., Schillings, M., Skipka, G. and Zange, J. (2001) Idebenone in patients with Friedreich ataxia. *Neurosci. Lett.,* **306,** 169-172.
40. Mariotti, C., Solari, A., Torta, D., Marano, L., Fiorentini, C. and Di Donato, S. (2003) Idebenone treatment in Friedreich patients: one-year-long randomized placebo-controlled trial. *Neurology,* **60,** 1676-1679.
41. Puccio, H., Simon, D., Cossee, M., Criqui-Filipe, P., Tiziano, F., Melki, J., Hindelang, C., Matyas, R., Rustin, P. and Koenig, M. (2001) Mouse models for Friedreich ataxia exhibit cardiomyopathy, sensory nerve defect and Fe-S enzyme deficiency followed by intramitochondrial iron deposits. *Nat. Genet.,* **27,** 181-186.
42. Simon, D., Seznec, H., Gansmuller, A., Carelle, N., Weber, P., Metzger, D., Rustin, P., Koenig, M. and Puccio, H. (2004) Friedreich ataxia mouse models with progressive cerebellar and sensory ataxia reveal autophagic neurodegeneration in dorsal root ganglia. *J. Neurosci.,* **24,** 1987-1995.
43. Seznec, H., Simon, D., Monassier, L., Criqui-Filipe, P., Gansmuller, A., Rustin, P., Koenig, M. and Puccio, H. (2004) Idebenone delays the onset of cardiac functional alteration without correction of Fe-S enzymes deficit in a mouse model for Friedreich ataxia. *Hum. Mol. Genet.,* **13,** 1017-1024.
44. Pasternack, R.F., Banth, A., Pasternack, J.M. and Johnson, C.S. (1981) Catalysis of the disproportionation of superoxide by metalloporphyrins. III. *J. Inorg. Biochem.,* **15,** 261-267.
45. Day, B.J., Shawen, S., Liochev, S.I. and Crapo, J.D. (1995) A metalloporphyrin superoxide dismutase mimetic protects against paraquat-induced endothelial cell injury, in vitro. *J. Pharmacol. Exp. Ther.,* **275,** 1227-1232.
46. Day, B.J., Fridovich, I. and Crapo, J.D. (1997) Manganic porphyrins possess catalase activity and protect endothelial cells against hydrogen peroxide-mediated injury. *Arch. Biochem. Biophys.,* **347,** 256-262.
47. Szabo, C., Day, B.J. and Salzman, A.L. (1996) Evaluation of the relative contribution of nitric oxide and peroxynitrite to the suppression of mitochondrial respiration in immunostimulated macrophages using a manganese mesoporphyrin superoxide dismutase mimetic and peroxynitrite scavenger. *FEBS Lett.,* **381,** 82-86.

48. Milano, J. and Day, B.J. (2000) A catalytic antioxidant metalloporphyrin blocks hydrogen peroxide-induced mitochondrial DNA damage. *Nucleic Acids Res.,* **28,** 968-973.
49. Patel, M.N. (2003) Metalloporphyrins improve the survival of Sod2-deficient neurons. *Aging Cell,* **2,** 219-222.
50. Melov, S., Coskun, P., Patel, M., Tuinstra, R., Cottrell, B., Jun, A.S., Zastawny, T.H., Dizdaroglu, M., Goodman, S.I., Huang, T.T. *et al.* (1999) Mitochondrial disease in superoxide dismutase 2 mutant mice. *Proc. Natl. Acad. Sci. U S A,* **96,** 846-851.
51. Melov, S., Doctrow, S.R., Schneider, J.A., Haberson, J., Patel, M., Coskun, P.E., Huffman, K., Wallace, D.C. and Malfroy, B. (2001) Lifespan extension and rescue of spongiform encephalopathy in superoxide dismutase 2 nullizygous mice treated with superoxide dismutase-catalase mimetics. *J. Neurosci.,* **21,** 8348-8353.
52. Epstein, C.J., Avraham, K.B., Lovett, M., Smith, S., Elroy-Stein, O., Rotman, G., Bry, C. and Groner, Y. (1987) Transgenic mice with increased Cu/Zn-superoxide dismutase activity: animal model of dosage effects in Down syndrome. *Proc. Natl. Acad. Sci. U S A,* **84,** 8044-8048.
53. Eisenstein, R.S. (2000) Iron regulatory proteins and the molecular control of mammalian iron metabolism. *Annu. Rev. Nutr.,* **20,** 627-662.
54. Torti, F.M. and Torti, S.V. (2002) Regulation of ferritin genes and protein. *Blood,* **99,** 3505-3516.
55. Lodi, R., Hart, P.E., Rajagopalan, B., Taylor, D.J., Crilley, J.G., Bradley, J.L., Blamire, A.M., Manners, D., Styles, P., Schapira, A.H. *et al.* (2001) Antioxidant treatment improves in vivo cardiac and skeletal muscle bioenergetics in patients with Friedreich's ataxia. *Ann. Neurol.,* **49,** 590-596.
56. Rong, Y., Doctrow, S.R., Tocco, G. and Baudry, M. (1999) EUK-134, a synthetic superoxide dismutase and catalase mimetic, prevents oxidative stress and attenuates kainate-induced neuropathology. *Proc. Natl. Acad. Sci. U S A,* **96,** 9897-9902.
57. Jung, C., Rong, Y., Doctrow, S., Baudry, M., Malfroy, B. and Xu, Z. (2001) Synthetic superoxide dismutase/catalase mimetics reduce oxidative stress and prolong survival in a mouse amyotrophic lateral sclerosis model. *Neurosci. Lett.,* **304,** 157-160.
58. Melov, S., Ravenscroft, J., Malik, S., Gill, M.S., Walker, D.W., Clayton, P.E., Wallace, D.C., Malfroy, B., Doctrow, S.R. and Lithgow, G.J. (2000) Extension of life-span with superoxide dismutase/catalase mimetics. *Science,* **289,** 1567-1569.
59. Patel, M. and Day, B.J. (1999) Metalloporphyrin class of therapeutic catalytic antioxidants. *Trends Pharmacol. Sci.,* **20,** 359-364.

60. Hinerfeld, D., Traini, M.D., Weinberger, R.P., Cochran, B., Doctrow, S.R., Harry, J. and Melov, S. (2004) Endogenous mitochondrial oxidative stress: neurodegeneration, proteomic analysis, specific respiratory chain defects, and efficacious antioxidant therapy in superoxide dismutase 2 null mice. *J. Neurochem.,* **88,** 657-667.
61. Shin, J.H., London, J., Le Pecheur, M., Hoger, H., Pollak, D. and Lubec, G. (2004) Aberrant neuronal and mitochondrial proteins in hippocampus of transgenic mice overexpressing human Cu/Zn superoxide dismutase 1. *Free Radic. Biol. Med.,* **37,** 643-653.
62. Turrens, J.F. (2001) Increased superoxide dismutase and Down's syndrome. *Med. Hypotheses,* **56,** 617-619.
63. Lee, M., Hyun, D.H., Halliwell, B. and Jenner, P. (2001) Effect of overexpression of wild-type and mutant Cu/Zn-superoxide dismutases on oxidative stress and cell death induced by hydrogen peroxide, 4-hydroxynonenal or serum deprivation: potentiation of injury by ALS-related mutant superoxide dismutases and protection by Bcl-2. *J. Neurochem.,* **78,** 209-220.
64. Tsuji, Y., Ayaki, H., Whitman, S.P., Morrow, C.S., Torti, S.V. and Torti, F.M. (2000) Coordinate transcriptional and translational regulation of ferritin in response to oxidative stress. *Mol. Cell Biol.,* **20,** 5818-5827.
65. Pietsch, E.C., Chan, J.Y., Torti, F.M. and Torti, S.V. (2003) Nrf2 mediates the induction of ferritin H in response to xenobiotics and cancer chemopreventive dithiolethiones. *J. Biol. Chem.,* **278,** 2361-2369.
66. MacEvilly, C.J. and Muller, D.P. (1997) Oxidative stress does not appear to be involved in the aetiology of Friedreich's ataxia. *Res. Neurol. Neurosci.,* **11,** 131-137.
67. Strain, J., Lorenz, C.R., Bode, J., Garland, S., Smolen, G.A., Ta, D.T., Vickery, L.E. and Culotta, V.C. (1998) Suppressors of superoxide dismutase (SOD1) deficiency in Saccharomyces cerevisiae. Identification of proteins predicted to mediate iron-sulfur cluster assembly. *J. Biol. Chem.,* **273,** 31138-31144.
68. Jensen, L.T., Sanchez, R.J., Srinivasan, C., Valentine, J.S. and Culotta, V.C. (2004) Mutations in Saccharomyces cerevisiae iron-sulfur cluster assembly genes and oxidative stress relevant to Cu,Zn superoxide dismutase. *J. Biol. Chem.,* **279,** 29938-29943.
69. Tan, G., Napoli, E., Taroni, F. and Cortopassi, G. (2003) Decreased expression of genes involved in sulfur amino acid metabolism in frataxin-deficient cells. *Hum. Mol. Genet.,* **12,** 1699-1711.
70. Vattem, K.M. and Wek, R.C. (2004) Reinitiation involving upstream ORFs regulates ATF4 mRNA translation in mammalian cells. *Proc. Natl. Acad. Sci. U S A,* **101,** 11269-11274.

71. Roybal, C.N., Yang, S., Sun, C.W., Hurtado, D., Vander Jagt, D.L., Townes, T.M. and Abcouwer, S.F. (2004) Homocysteine increases the expression of vascular endothelial growth factor by a mechanism involving endoplasmic reticulum stress and transcription factor ATF4. *J. Biol. Chem.,* **279,** 14844-14852.

72. Hegde, P., Qi, R., Abernathy, K., Gay, C., Dharap, S., Gaspard, R., Hughes, J.E., Snesrud, E., Lee, N. and Quackenbush, J. (2000) A concise guide to cDNA microarray analysis. *Biotechniques,* **29,** 548-554.

LEGENDS TO FIGURES

Figure 1: MnSOD mimetic therapy and Cu,ZnSOD overexpression has no beneficial effect on the murine FRDA cardiomyopathy.

A). Kaplan-Meier survival curve of MnTBAP-treated Frda/MCK mutant animals (full line) compared to placebo mutant littermates (dotted line) (Mantel-Cox Logrank p=0,099). B). Kaplan-Meier survival curve of L3/L-; MCK-Cre^{+}; SOD1^{+} (full line) compared to L3/L-; MCK-Cre^{+} animals (dotted line) (Mantel-Cox Logrank p=0,45).

Figure 2: Absence od oxidative stress and decrease of superoxide dismutase expression in frataxin-deficient tissues

A). Quantitative-RTPCR and western blot analysis performed on whole heart mRNA and protein extracts of Frda/MCK mutants showing a modest MnSod induction between 2 to 7 weeks following by a dramatic decrease (8 and 10 weeks). Representative western blot are shown. B). Quantitative-RTPCR and western blot analysis performed on whole cerebellum mRNA and protein extracts of Frda/Prp mutants showing progressive MnSod decrease between 5 and 20 weeks. Representative western blot are shown. C). Quantitative-RTPCR of frataxin gene performed on whole cerebellum mRNA of Frda/Prp mutants. Results are expressed as a percentage of frataxin expression level in control littermate mice with normal frataxin level. Frataxin levels are restored, following the loss of the frataxin negative neurons. D). Protein oxidation status assessed by OxyBlot in total cerebellum extracts of Frda/Prp mutants from 5 to 40 weeks, expressed as a percentage of oxidized protein level in control littermate mice. Protein and cDNA levels are normalized using β-tubulin and murine Hprt as internal standards, respectively. C= control; M= mutant. Statistical analysis was done by Student T test, *p<0,05, **p<0,01, ***p<0,001.

Figure 3: IRP1/Aconitase activity in Frda/MCK mutants

Cytosolic extracts from the heart of wild type and Frda/MCK mutant mice at the age of 5, 8 and 10 weeks were analysed. A) cytosolic aconitase activity and B) IRP-1/IRE binding activity in the presence or absence of 2% 2-mercaptoethanol (2-ME) were measured (in each sample) by spectrophotometry and gel mobility shift assay, respectively. C). Radioactivity associated with IRP-1/IRE complexes was quantified by PhosphorImaging. IRP-1 activity was expressed as a percentage of the value obtained after exposure to 2%-ME, which allows visualization of the total IRE binding activity of IRP-1.

Figure 4: Iron homeostasis and gene expression in heart of Frda/MCK animals.

A. Gene expression in heart between 2 and 10 weeks are represented as a percentage of expression level in control littermate mice with normal frataxin level. cDNA levels are normalized using murine Hprt. Black box, IRP-1; grey box, IRP-2; streaked box, transferrin receptor; white dotted box, ferritin L; black dotted box, ferritin H.

Statistical analysis was done by Student T test, *p<0,05, **p<0,01, ***p<0,001.

B. Cytosolic L-ferritin expression in the heart of wild type and Frda/MCK mice at the age of 5, 8 and 10 weeks. Equal amount of protein (30 mg) were analyzed by Western blot analysis using an anti-ferritin antisera or a mouse monolonal anti-vinculin antibody as a loading control. Purified L-ferritin from mouse liver and cytosolic extracts from iron-treated RAW 264.7. Macrophages were used as positive control. FAC, ferric ammonium citrate. D, deferrioxamine.

Figure 5: Quantitative-RTPCR analysis of differentially expressed genes from 'MitoChips' experiments.

Gene expression in heart between 2 and 10 weeks are represented as a percentage of expression level in control littermate mice with normal frataxin level. cDNA levels are normalized using murine Hprt. A). Black box, Mthfd2 (note that at 2 weeks, the relative expression is already 150% of wildtype). Grey box, Asparagine synthetase B). Black box, asparaginyl-tRNA synthetase. Grey box, Glutamyl-tRNA synthetase. C). Black box, Glutathione S-transferase like omega 1. Grey box, Cathepsin L. Streaked box, ATPase H. Statistical analysis was done by Student T test, *p<0,05, **p<0,01, ***p<0,001.

Table 1
Alterations in gene expression of Frda/MCK mutant mice as compared with control littermate mice.

GenBank Number	Gene Name	Gene Expression Changes (Mean)
BG076333	Mthfd2	7.2 +
BG088553	Asparagine synthetase	4.1 +
BG084006	Glutathione S-transferase omega 1-like	2.5 +
BG078497	Cathepsin L	2.3 +
BG064794	Ferritin L	2.0 +
BG086960	vacuolar ATPase subunit H	2.0 +
BG088535	Glutamyl-tRNA synthetase	1.9 +
BG065221	Ornithine decarboxylase	1.7 +
BG070855	Glycogenin 1	1.7 +
NM_009082	Ribosomal protein L29	1.6 +
BG073196	Collagen pro-alpha-1	1.6 +
BG079401	Asparaginyl-tRNA synthetase	1.6 +
BG064735	Peroxiredoxin 5	1.6 +
BG087383	Cathepsin D	1.6 +
BG067699	Interferon-related developmental regulator 1	1.6 +
BG080951	Alanyl-tRNA synthetase	1.5
BG070116	Guanine nucleotide binding protein, beta-2, related sequence 1	1.5 +
BG083822	Cytochrome c oxidase subunit VIaL	1.5 +
BG077385	Protease 26S ATPase 5	1.4 +
BG064035	Phosphoprotein enriched in astrocytes 15	1.4 +
BG076060	NADH dehydrogenase (NDUFS3)	1.1 -
NM_008044	Frataxin	1.2 -
BG063515	Ferritin heavy chain	1.2 -
BG087262	NADH dehydrogenase (NDUFS2)	1.2 -
BG088100	NADH dehydrogenase (NDUFS1)	1.2 -
BG073718	Glutathione peroxidase 3	1.4 -
BG086391	Cytosolic acyl coenzyme A thioester hydrolase	1.4 -
BG072288	Adenylyl cyclase type 9	1.5 -
BG072299	Receptor (calcitonin) activity modifying protein 2	1.5 -
BG085195	ATPase, Ca++ transporting cardiac muscle, slow twitch 2	1.8 -

GenBank Accession numbers are shown on the left. Means of gene expression changes in seven independent experiments are shown on the right. + and - indicate increased and decreased gene expression in the Frda/MCK heart mutant, respectively.

Figure 1

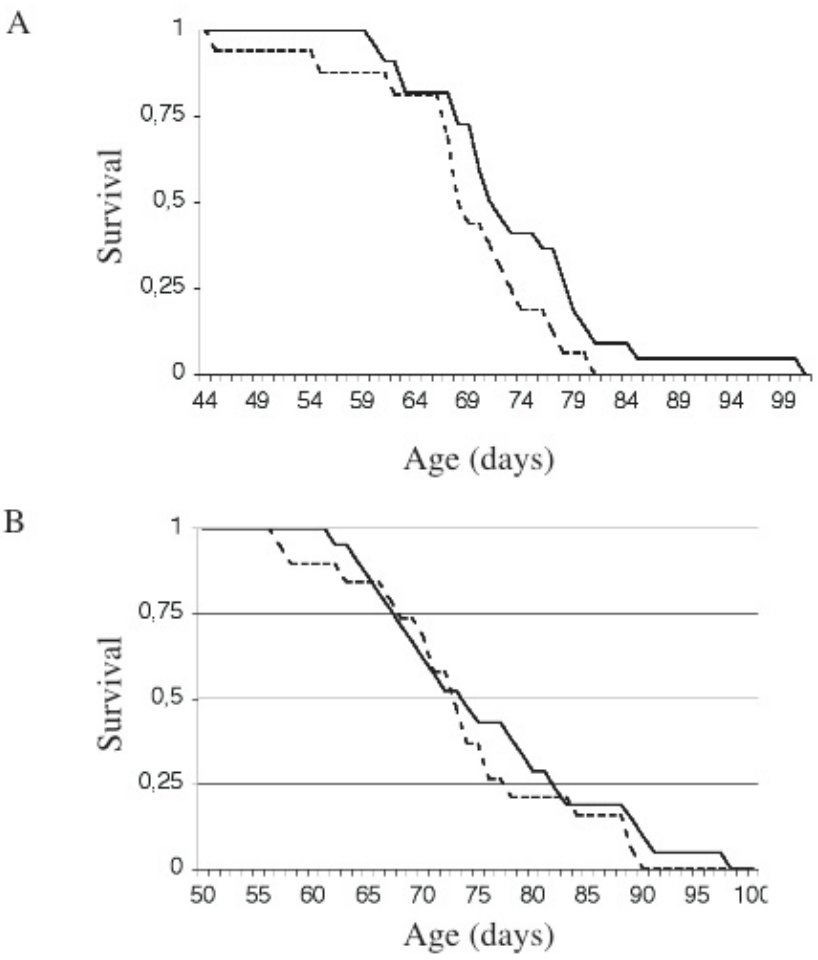
A
1
0,75
0,5
0,25
0
Survival
44 49 54 59 64 69 74 79 84 89 94 99
Age (days)
B
1
0,75
0,5
0,25
0
Survival
50 55 60 65 70 75 80 85 90 95 100
Age (days)

Figure 2

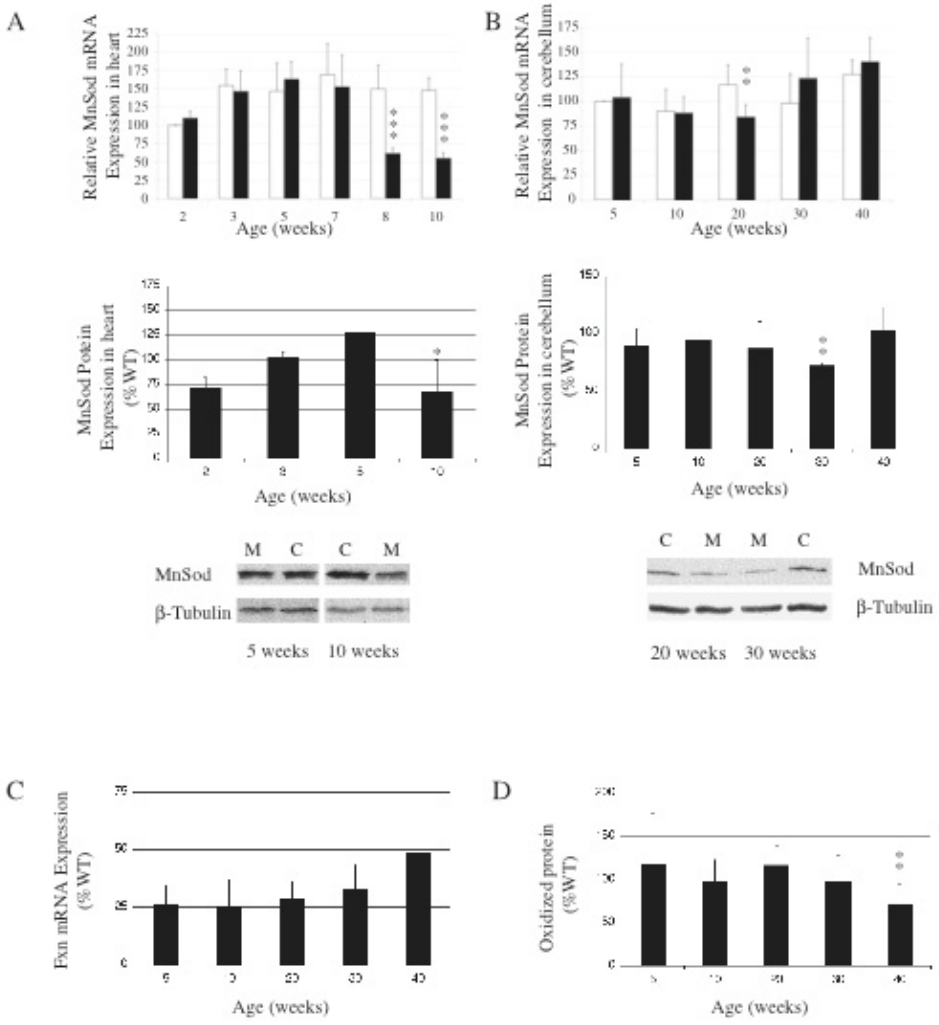
A
Relative MnSod mRNA Expression in heart
Age (weeks)
MnSod Protein Expression in heart (% WT)
Age (weeks)
M C C M
MnSod
β-Tubulin
5 weeks 10 weeks
B
Relative MnSod mRNA Expression in cerebellum
Age (weeks)
MnSod Protein Expression in cerebellum (% WT)
Age (weeks)
C M M C
MnSod
β-Tubulin
20 weeks 30 weeks
C
Fxn mRNA Expression (% WT)
Age (weeks)
D
Oxidized protein (% WT)
Age (weeks)

Figure 3

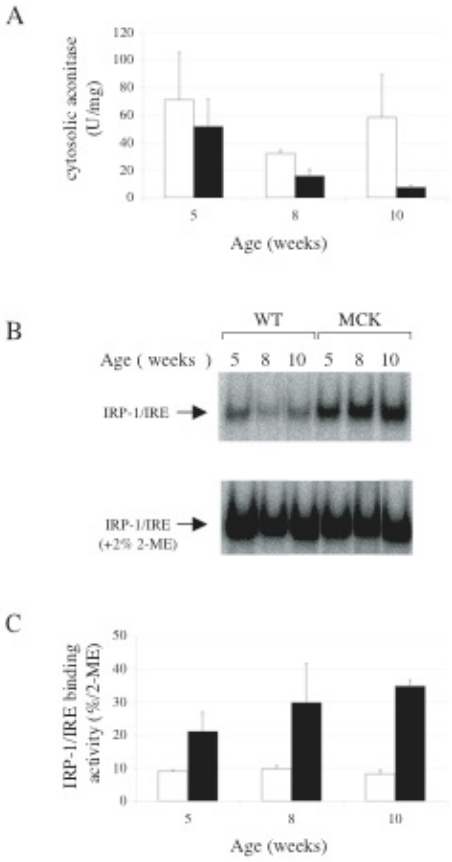
A
cytosolic aconitase (U/mg)
120
100
80
60
40
20
0
5
8
10
Age (weeks)
B
WT
MCK
Age (weeks) 5 8 10 5 8 10
IRP-1/IRE
IRP-1/IRE (+2% 2-ME)
C
IRP-1/IRE binding activity (%/2-ME)
50
40
30
20
10
0
5
8
10
Age (weeks)

Figure 4

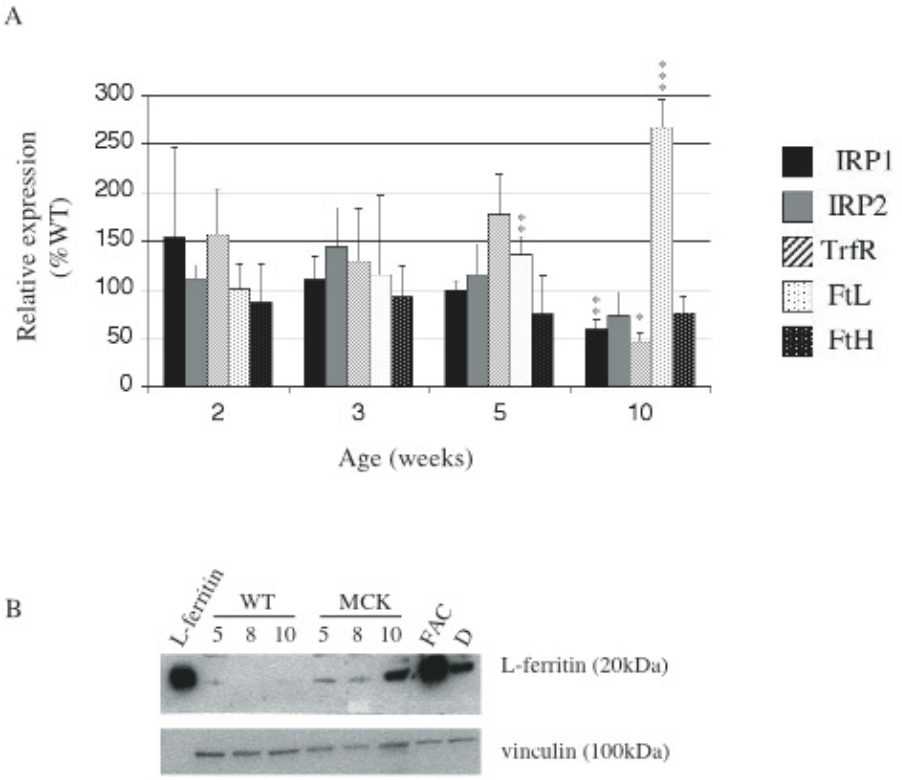
A
Relative expression (%WT)
300
250
200
150
100
50
0
2
3
5
10
Age (weeks)
IRP1
IRP2
TrfR
FtL
FtH
B
L-ferritin
WT
MCK
5 8 10 5 8 10
FAC
D
L-ferritin (20kDa)
vinculin (100kDa)

Figure 5

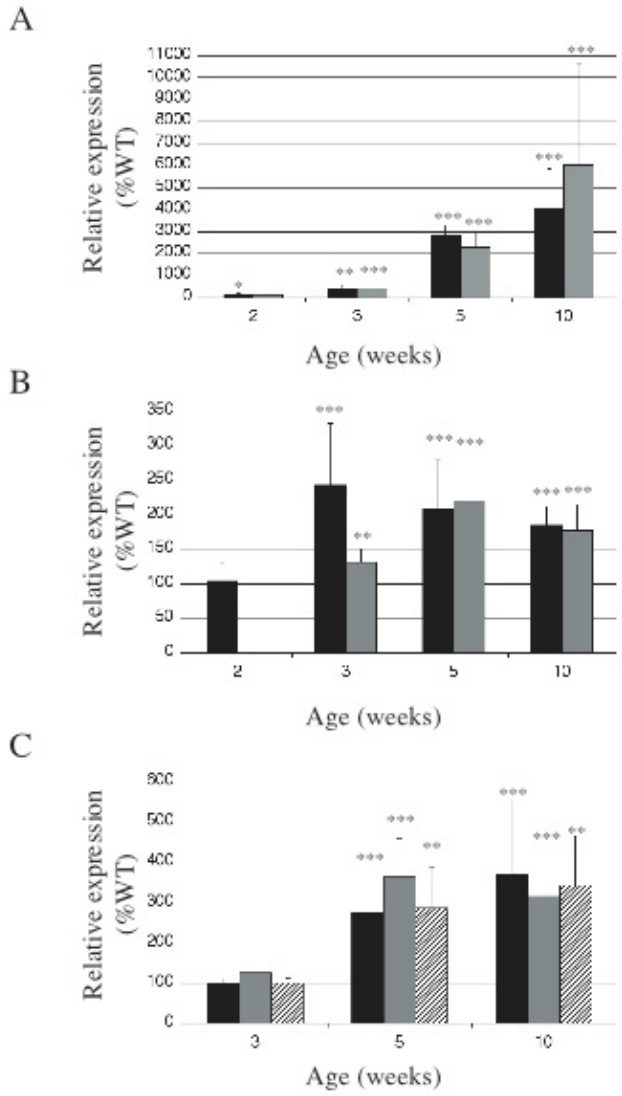
A
Relative expression (%WT)
11000
10000
9000
8000
7000
6000
5000
4000
3000
2000
1000
0
2
3
5
10
Age (weeks)
B
Relative expression (%WT)
350
300
250
200
150
100
50
0
2
3
5
10
Age (weeks)
C
Relative expression (%WT)
600
500
400
300
200
100
0
3
5
10
Age (weeks)

ABBREVIATIONS

FRDA, Friedreich ataxia; ISC, iron-sulfur cluster ; MCK, muscle creatine kinase; PrP, Prion Protein; MnSod and Sod2, Manganese superoxide dismutase.